



Sharif University of Technology

Scientia Iranica

Transactions C: Chemistry and Chemical Engineering

www.sciencedirect.com



# Preparation and characterization of visible light sensitive nano titanium dioxide photocatalyst

H.S. Mazloomi Tabaei, M. Kazemeini\*, M. Fattahi

Department of Chemical and Petroleum Engineering, Sharif University of Technology, Tehran, P.O. Box 11365-9465, Iran

Received 25 September 2011; revised 22 April 2012; accepted 22 May 2012

## KEYWORDS

Photocatalyst;  
TiO<sub>2</sub>;  
Visible light;  
Dye sensitization;  
Anatase;  
Rutile.

**Abstract** Dye sensitizers loaded on TiO<sub>2</sub> decrease the electron excitation energy, thereby improving the photocatalytic performance by causing an increase in sensitivity under visible light irradiation. Three dye sensitizer precursors, Mordant Orange 1, N<sub>3</sub> (red dye) and Cobalt (II) Phthalocyanine Tetrasulfonate (CoPcTs), were utilized to load the photocatalyst. The rate of the electron trapping process on platinum is clearly compatible with the migration rate of boundary electrons. Consequently, the migration of boundary electrons from the conduction band towards electron acceptors is increased by loading platinum onto the titanium dioxide.

In this research, TiO<sub>2</sub> was synthesized from a titanium isopropoxide precursor using the sol-gel method, and the product was compared with commercial TiO<sub>2</sub>-P25 (consisting of 80% anatase and 20% rutile phases). Evaluation of the effect of calcination temperature on the formation of the nanosize photocatalyst and the phase formed was performed through the XRD technique. The specific surface area was determined by BET measurement. Ultimately, the absorption of all samples and their efficiencies were compared using the Diffuse Reflectance Spectroscopy (DRS) technique under visible light irradiation.

© 2012 Sharif University of Technology. Production and hosting by Elsevier B.V. All rights reserved.

## 1. Introduction

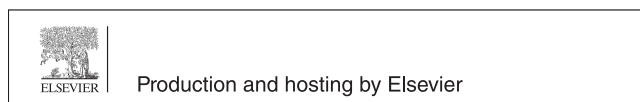
Titanium dioxide has received attention due to its properties of chemical stability, non-toxicity, and photocatalytic characteristics concerning environmental pollution [1].

The photocatalytic phenomenon may be frequently observed in the dye degradation of external walls of buildings over time as a result of oxidation. For example, TiO<sub>2</sub> particles are currently used in dyes, and degradation of organic molecules present in the dye occurs when part of the applied solar energy irradiates the dye layer [2]. Therefore, vast amounts of research have been conducted concerning the use of this phenomenon for the purification of water, air, and soil contaminated with toxic agents [2–8]. Since the 1980s, photocatalytic purification of water has been proposed as an alternative for removing pollutants from water [9].

The distinction between a nanoparticle and particles larger than 100 nanometers is that nanoparticles possess no charge within them, but create a strong electric field, while larger particles possess a charge layer under the surface and one in a central zone [10]. Therefore, when larger particles are exposed to incident light, the surface will be occupied by holes. Thus, instead of migrating towards the surface, electrons will accumulate in the particle center because of the barrier caused by Schottky structural defects (i.e., a Schottky bond forms when a semiconductor is in contact with other materials having a variable surface form). Hence, holes and electrons are inhibited from taking part in the redox reaction, with water and dissolved oxygen, to produce active oxygen agents, which leads to a reduction in the photocatalytic yield of macro-relative to nanoparticles. Generally, the smaller the size of TiO<sub>2</sub> particles, the faster the holes and electrons generated by incident light will migrate toward the surface and the more active centers are formed on the nanoparticle surface. Furthermore, the generated electrons do not combine conveniently with holes due to the very large area to volume ratio. This lag in recombination of holes and electrons results in an increase in photocatalytic efficiency [11,12]. Hence, the aim of this research is to approach this effect through the production and utilization of TiO<sub>2</sub> nanoparticles.

\* Corresponding author. Tel.: +98 21 66165425.

E-mail addresses: h\_mazloomi@yahoo.com (H.S.M. Tabaei), kazemeini@sharif.edu (M. Kazemeini), moslem.fattahi@gmail.com (M. Fattahi).  
Peer review under responsibility of Sharif University of Technology.



In order to compare the performance of modified titanium dioxides and their activities in visible light, a study of their influences in reducing contamination of Methyl Tertiary Butyl Ether (MTBE) takes place. This substance has replaced tetra ethyl lead in gasoline since 1970, and is widely used in unleaded gasoline in some countries in order to increase its octane rating. Evaluation of the problems caused by consumption of this substance has led to enforcement of restrictions on its usage. Nanotechnology has the potential to play a unique role in tackling the environmental crisis through its ability to purify water sources contaminated with MTBE, and to decompose it to dissoluble biological products. In order to achieve these goals, the developed oxidation process, based upon modified photocatalysts of synthesized  $\text{TiO}_2$  exposed to visible light, might be used.

Utilization of the titanium dioxide photocatalyst has been restricted due to the low quantum yield and the use of ultraviolet rays, in other words, lack of visible light. Photocatalysts are often used when adding metals or other hole trapping agents to increase the lifetime of excitations created. This means the life of excited electrons and holes as adequate traps should be increased to reduce their recombination effectively. Introducing group VIII metals onto  $\text{TiO}_2$  to improve photocatalytic activity has been frequently investigated [13–19]. Loading of these metals onto  $\text{TiO}_2$  increases the photocatalytic reaction rate due to the trapping of conduction band electrons followed by elevation of electron-hole pair lifetimes [20]. In much research, platinum was reported to be the most active metal of group VIII for increasing  $\text{TiO}_2$  activity. The trapping of electrons into the platinum phase happens during a  $1\ \mu\text{s}$  period [21], thus, migration of boundary electrons towards the sensitizer occurs at around the same period of  $1\ \mu\text{s}$  [22]. Therefore, the rate of electron trapping on platinum is comparable with the rate of boundary electron migration. Consequently, migration of boundary electrons in the conduction band towards electron acceptors increases with enhanced loading of platinum onto the  $\text{TiO}_2$ .

Ordinarily, both anatase and rutile phases are present in synthesized crystals of  $\text{TiO}_2$ , and the difference in the lattice structure of the aforementioned phases leads to a difference in mass density (i.e., rutile with  $\rho = 4.25\ \text{g/cm}^3$  and anatase with  $\rho = 3.894\ \text{g/cm}^3$ ) and the electron bond configuration between them. Thus, recombination of electron-hole pairs created by irradiation on the surface of the rutile phase occurs faster, and the amount of reactants and hydroxyls bonded to this surface is smaller than at the surface of the anatase phase. Therefore, as mentioned in some research in the open literature, the greater the amount of anatase in the  $\text{TiO}_2$  sample, the higher the photocatalytic activity [1,2,9,11,12,23–25]. However, the anatase phase is unstable and converts to the rutile phase irreversibly. Hence, many properties of nanocrystal arise from anatase and its lifetime in the nanocrystal [26].

Because of the high band gap of titanium dioxide, this substrate requires high energy absorption for excitation, electron donation, and consequent recovery of pollutant. Ultimately, it is inactive in the visible light region. Absorption in this range requires a semiconductor with a band energy less than, or equal to, 3 eV. However, the band energies of rutile and anatase phases are 3 and 3.2 eV, respectively. Furthermore, pure rutile is obtained from anatase by temperature elevation. High temperature gives a low specific surface area, and, hence, the low porosity of precipitated large sized  $\text{TiO}_2$  particles. However, rutile synthesis occurs with a high specific area via the sol-gel method at low temperature, based upon the long lifetime of sol

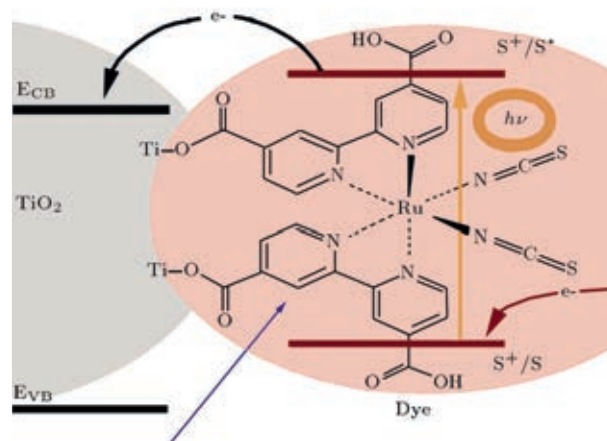


Figure 1: Schematic of the dye sensitization process.

tania with the stable rutile phase. In fact, the solubility and recrystallization of an oxide in the mother liquor leads to the formation of a crystal phase, which is more stable in comparison with anatase.

Exposure of a photocatalyst to light excites it by supplying its band gap energy. This creates electrons and holes or positive charge. These pairs either recombine, causing heat evolution, or lead to absorption of organic pollutants, hence, its purification. An increase in photocatalytic efficiency and utilization of visible light may be exhibited due to dye sensitization. The dye precursor is excited by the irradiation of light, and the electron transforms from the HOMO state into the excited state, and, thereafter, into the conduction band of the  $\text{TiO}_2$ . In fact, the conduction band of  $\text{TiO}_2$  is an intermediate for electron transfer from dye precursor to the material which is intended for elimination (Figure 1). This is depicted as follows:



Although much research has concentrated on activation of commercial titanium dioxide and the use of ultraviolet light, these rays occupy just 4% of the solar spectrum.

The objective of the present work is to shift activation from the UV range to the visible range, as a first step in eliminating the defects of the titanium dioxide photocatalyst. Visible light adsorption depends on utilization of semiconductors as a photocatalyst with a gap energy less than or equal to 3 eV. In order to clarify the role of the base  $\text{TiO}_2$  in a Pt-modified  $\text{TiO}_2$  photocatalyst, first, synthesis of a rutile  $\text{TiO}_2$  sample took place and, then, deposition of Pt onto this and  $\text{TiO}_2$  (Degussa P-25) samples was performed. Finally, the Pt-modified  $\text{TiO}_2$ -P25 was dye sensitized and compared with dye sensitized Pt-modified synthesized rutiles, with three samples of dye, in the visible light region.

## 2. Experimental

### 2.1. Characterization techniques

Thermal Gravimetry Analysis (TGA) of  $\text{TiO}_2$ -P25 for removal of PEG at 110 and 350 °C was performed, which confirmed the complete removal of PEG during the final treatment at 350 °C [27]. X-ray Diffraction (XRD) patterns of samples were recorded on a PW184 model (Philips Company), with  $\text{Cu K}\alpha$  radiation of wavelength 0.15406 nm, and were analyzed from 15°

to  $75^\circ$  ( $2\theta$ ), with a step size of  $0.05^\circ$ , to assess crystallinity and confirm the phase structure. The crystallite size was estimated by line broadening utilizing the Scherrer equation. Porosimetry analysis (Quantasorb Instrument from Quantachrome Company) was used at liquid nitrogen temperature (77 K) to measure the Brunauer–Emmett–Teller (BET) specific surface area using nitrogen adsorption–desorption isotherms. At room temperature, diffuse reflectance spectroscopy (DRS) was used for optical characterization of  $\text{TiO}_2$  nanoparticles. All spectra were taken in the range of 390–700 nm on the Tex Flash instrument (Data Color Company). Details of the DRS technique are presented elsewhere in [28].

From the XRD patterns, the ratio of anatase ( $x_A$ ) in the  $\text{TiO}_2$  samples was estimated using the following relation:

$$X_A = \frac{I_R/I_A \cdot 0.79}{1 + I_R/I_A \cdot 0.79}, \quad (3)$$

where  $I_A$  and  $I_R$  are the integral intensities of the anatase (101) and rutile (110) reflections, respectively. The average size of the individual crystal size of  $\text{TiO}_2$  ( $d$ -spacing) was calculated by means of Scherrer's equation, i.e.:

$$d = \frac{0.9\lambda}{\beta \cos \theta}, \quad (4)$$

where  $\lambda$  is the X-ray wavelength corresponding to Cu  $K_\alpha$  radiation (0.15406 nm),  $\beta$  is the broadening (in radians) of the anatase (101) reflection, and  $\theta$  is the angle of diffraction corresponding to the peak broadening [29].

## 2.2. Synthesis of $\text{TiO}_2$ effective in visible light in the form of rutile phase

Titanium isopropoxide (obtained from the TIP, Fluka Purum, Switzerland) as precursor is initially hydrolyzed under mixing, by addition of isopropanol (dehumidified by sodium slices) and hydrochloric acid (with a ratio of 23.5  $\text{cm}^3$  hydrochloric acid and 3.78  $\text{cm}^3$  isopropanol for each 14  $\text{cm}^3$  of TIP). The role of isopropanol and hydrochloric acid is to control the hydrolysis rate. It should be noted that hydrolysis is carried out under conditions of vacuum and nitrogen gas flow at  $75^\circ\text{C}$ .

After the formation of hydrosol, during 48 h at room temperature, polyethylene glycol (50 mg/ml, PEG-4000) was added to it while mixing in order to control the size of crystal pores. The resultant mixture was dried at room temperature. It was subsequently calcinated at a temperature of  $110^\circ\text{C}$  for 24 h, and then, after the temperature rose to  $450^\circ\text{C}$ , at a heating rate of  $2^\circ\text{C}/\text{min}$ , was kept there for 6 h. Ultimately, the applied rutile phase was called the synthesized sample, with a calcination temperature of  $450^\circ\text{C}$ , containing 83% rutile phase.

## 2.3. Preparation of Pt/ $\text{TiO}_2$ photocatalyst

In order to deposit platinum onto the  $\text{TiO}_2$  and, thereby, improve the photocatalytic performance in the visible light range, first, 13  $\text{cm}^3$  of 0.01 molar hexachloroplatinic acid solution ( $\text{H}_2\text{PtCl}_6$ ) was made up to 26  $\text{cm}^3$  with water, and then, 2.5 g of synthesized  $\text{TiO}_2$  powder was added to it. After mixing for over 0.5 h, a solution obtained from mixing 0.07 g  $\text{NaBH}_4$  (Merck) into 10  $\text{cm}^3$  of water was introduced to achieve effective platinum diffusion through  $\text{TiO}_2$  pores. The resultant slurry was grayish in color. The sample was filtered, washed, and then kept at a temperature of  $75^\circ\text{C}$  over a period of 12 h. The calcinated temperature of  $350^\circ\text{C}$  for 24 h was applied for all samples with  $\text{TiO}_2$ . Thus, loaded platinum onto the  $\text{TiO}_2$  (i.e., Pt/ $\text{TiO}_2$ ) was obtained. Titanium dioxide synthesized in these studies was compared with commercial  $\text{TiO}_2$ -P25 powder made by Degussa (Germany).

## 2.4. Modifying $\text{TiO}_2$ via $\text{N}_3$ sensitization

One of the most ordinary and effective dye sensitizers loaded onto the titanium dioxide is the Red Ruthenium complex, typically indicated by  $\text{Ru}^{\text{II}}(2, 2'\text{-bipyridyl-4, 4'}\text{-dicarboxylate})_2\text{-(NCS)}_2$ , known as  $\text{N}_3$ , obtained from Solaronix of Switzerland. Three grams of synthesized  $\text{TiO}_2$  powder were added to 30  $\text{cm}^3$  of aqueous  $\text{N}_3$  (3.7% ethanol by weight to volume ratio) mother solution and kept at room temperature for 24 h. The sample was then filtered and washed until discoloration occurred. It was maintained at a temperature of  $100^\circ\text{C}$  for over 15 min. The obtained synthesized  $\text{TiO}_2$  loaded by  $\text{N}_3$  (i.e.,  $\text{N}_3/\text{TiO}_2$ ) was kept in a desiccator till used.

## 2.5. Modifying $\text{TiO}_2$ via Mordant sensitization

Since Red Ruthenium is a rare metal and its complexes are not recoverable, Mordant sensitizers are used commercially. Three grams of synthesized  $\text{TiO}_2$  powder were added to 25  $\text{cm}^3$  of cupric color Mordant mother solution (50% water weight to volume ratio) to give an orange solution. The sample was kept in a bath at  $100^\circ\text{C}$  for 2 h and then filtered and washed (with water and, thereafter, methanol) until discoloration occurred. The sample was dried at a temperature of  $80^\circ\text{C}$  in an oven. The ethanol used in the aforementioned sensitizations had 99.5% purity.

## 2.6. Modifying $\text{TiO}_2$ via CoPcTs sensitization

CoPcTs is another dye sensitizer that was synthesized and utilized for comparison with the above two samples. One gram of synthesized  $\text{TiO}_2$  was added to the CoPcTs solution (0.02 g of powder CoPcTs in 100  $\text{cm}^3$  of water) and mixed in the dark over a period of 12 h. Then, it was filtered and washed. The sample was dried at a temperature of  $75^\circ\text{C}$  in an oven for one night and kept in the dark.

## 2.7. Some other methods of modifying $\text{TiO}_2$ photocatalyst

In order to investigate the influence of the rutile phase in improving the photocatalytic properties of  $\text{TiO}_2$ , the synthesized  $\text{TiO}_2$  sample in the rutile phase was used, and dye precursors sensitive to light, including Mordant Orange 1,  $\text{N}_3$ , CoPcTs and Pt metal, were loaded onto it. As a result, Mordant/Rutile,  $\text{N}_3$ /Rutile, CoPcTs/Rutile, and Pt/Rutile were obtained. Again, to study the role of platinum, dye precursors which were sensitive to light were loaded onto Pt/ $\text{TiO}_2$  (i.e., amount of platinum is one percent) and, hence,  $\text{N}_3$ /Pt/ $\text{TiO}_2$ , Mordant/Pt/ $\text{TiO}_2$ , and CoPcTs/Pt/ $\text{TiO}_2$  were obtained. Details of these sample preparations are provided in the following.

Three grams of synthesized Pt/ $\text{TiO}_2$  powder were added to 10  $\text{cm}^3$  of aqueous  $\text{N}_3$  (3.7% ethanol by weight to volume ratio) mother liquor. The 10  $\text{cm}^3$  of ethanol were added to this solution and kept at room temperature for 24 h. The sample was then filtered and washed until discoloration occurred. It was maintained at a temperature of  $100^\circ\text{C}$  for over 15 min. The obtained synthesized Pt/ $\text{TiO}_2$  loaded by  $\text{N}_3$  (i.e.,  $\text{N}_3/\text{Pt}/\text{TiO}_2$ ) was kept in a desiccator till used.

On the other hand, three grams of synthesized Pt/ $\text{TiO}_2$  powder were added to 25  $\text{cm}^3$  of cupric color Mordant mother liquor (containing 50% in volume ratio) to give a dark solution. The sample was kept in a bath at  $80^\circ\text{C}$  for 2 h, and then filtered and washed (with water and, then, after, with methanol) until discoloration occurred. The sample was dried

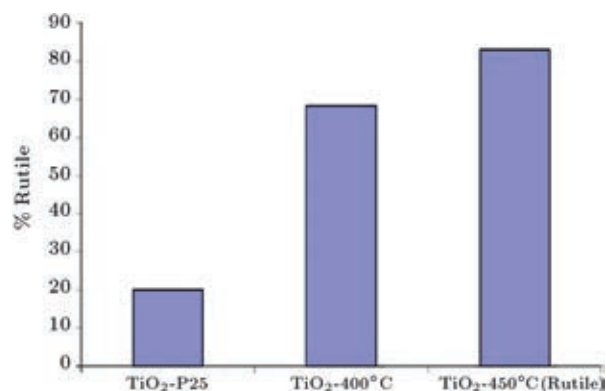


Figure 2: The influence of calcination temperature on rutile phase percentage.

at a temperature of 80 °C in an oven. The obtained material was Mordant/Pt/TiO<sub>2</sub>.

Ultimately, one gram of synthesized Pt/TiO<sub>2</sub> was added to the CoPcTs solution (containing 0.02 g of CoPcTs powder in 100 cm<sup>3</sup> of water) and mixed in the dark over a period of 12 h. Then it was filtered and washed. The sample was dried at a temperature of 75 °C in an oven for one night and kept in the dark. The obtained material was CoPcTs/Pt/TiO<sub>2</sub>.

### 3. Results and discussion

Titanium dioxide calcinated at a temperature of around 300–450 °C has an optimum specific surface area for formation of Ti–O–Pt bonds. Therefore, its photocatalytic adsorption and activity under irradiation of visible light are high [30]. Active rutile in visible light with a specific surface area of 65 m<sup>2</sup>/g was prepared by sol–gel synthesis at low temperature (450 °C), based upon the long residency of sol titania, due to the stability of the rutile phase. The rutile phase appears to be formed in hydrosol, along with the anatase phase, after a few hours, such that the rutile phase grows after 48 h. This is followed by calcination to remove polyethylene glycol (PEG). According to the XRD results indicated in Figure 2, the rutile phase reached 83%. These results show that there is no peak for anatase and rutile at the calcination temperature of 350 °C and the sample is still amorphous or non-crystalline (see Figure 3). Furthermore, Figure 3 indicates that with increasing crystallization temperature, an increase in the percentage of rutile phase compared to anatase is observed. It is noteworthy that ranges of the Bragg angle for the main TiO<sub>2</sub> phases, including rutile (27°, 36° and 54°) and anatase (25° and 47°), help to create a better understanding of the XRD patterns provided in this figure, in terms of the structure of the undertaken material. BET measurements shows an increase in the TiO<sub>2</sub> specific surface area from 50 m<sup>2</sup>/g for TiO<sub>2</sub>-P25 to 65 m<sup>2</sup>/g for the rutile phase in the synthesized TiO<sub>2</sub> sample (see Table 1). However, growth of particles is rather disadvantageous as it causes a reduction in absorption [31]. For example, it is seen that when the calcination temperature increases from 400 to 450 °C, the size of particles increases from 15.36 to 29.43 nm, according to evaluation of XRD patterns (see Table 1).

The loading of platinum on the rutile phase (Pt/Rutile) without changing the XRD pattern (therefore, without changing the percentage of the rutile phase), due to the uniform and adequate dispersion of Pt particles, improves particle size to

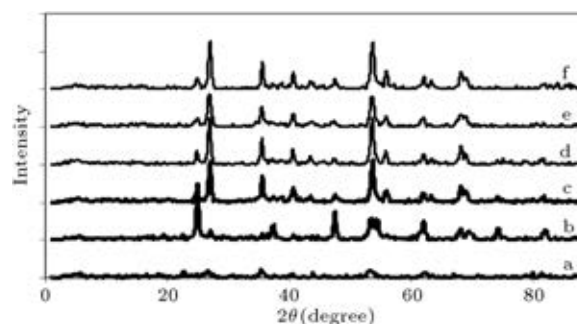


Figure 3: Comparison of the XRD patterns: (a) Synthesized TiO<sub>2</sub> with a calcination temperature of 350 °C, (b) Pt/TiO<sub>2</sub>-P25, (c) Pt/Rutile, (d) N<sub>3</sub>/Pt/Rutile, (e) synthesized TiO<sub>2</sub> with a calcination temperature of 400 °C and (f) synthesized TiO<sub>2</sub> with a calcination temperature of 450 °C (this sample is called “rutile” in this paper).

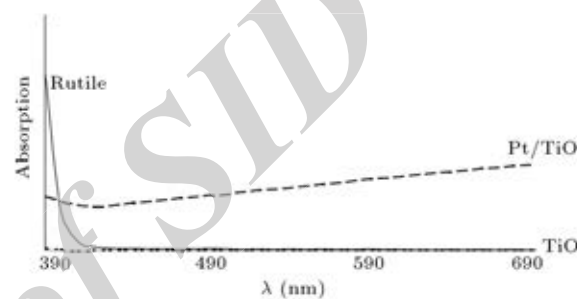


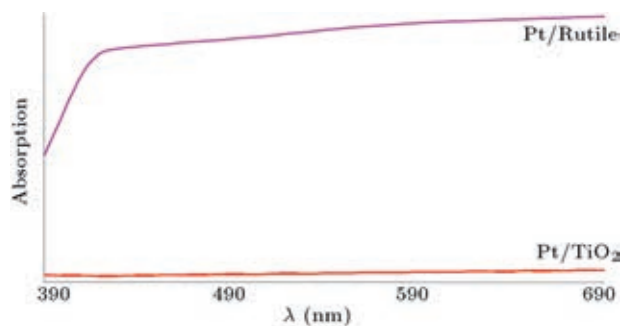
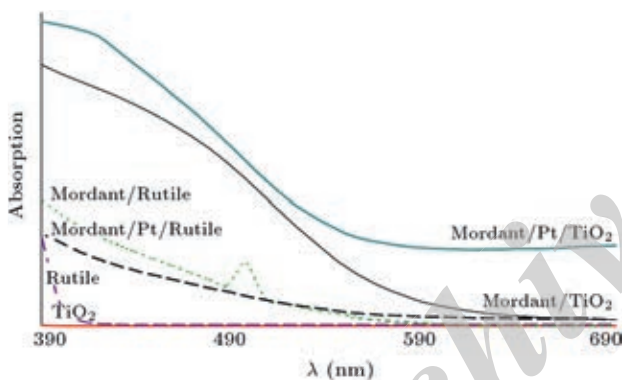
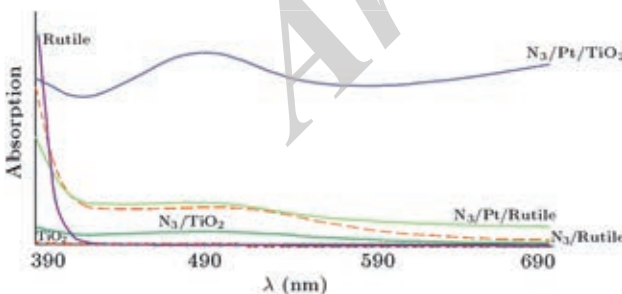
Figure 4: DRS comparison of TiO<sub>2</sub>-P25 (TiO<sub>2</sub>), synthesized TiO<sub>2</sub> with a calcination temperature of 450 °C (rutile) and TiO<sub>2</sub> loaded with Pt (Pt/TiO<sub>2</sub>).

22 nm. Loading dye sensitive N<sub>3</sub> on rutile modified with platinum (N<sub>3</sub>/Pt/Rutile) increases particle sizes to 23.8 nm. The effect of platinum loading onto the TiO<sub>2</sub> is observed in the form of a reduction of particle sizes to 20.58 nm (Table 1). Comparison of activities of synthesized photocatalysts in the visible light range was carried out by a light Diffuse Reflectance Spectroscopy (DRS) technique. Absorption in TiO<sub>2</sub>-P25 occurs in the UV range, while for the rutile phase, a slight absorption occurs in the visible light range (see Figure 4). The absorption of commercial TiO<sub>2</sub>-P25 under UV has been previously performed [32]. With the loading of platinum (Pt/TiO<sub>2</sub>), absorption occurred in the visible range. According to Figure 5, with synthesis of the TiO<sub>2</sub> sample in the rutile phase and the loading of platinum onto it (Pt/Rutile), the amount of absorption in the visible range is considerably greater than that of the Pt/TiO<sub>2</sub>. However, in both cases, maximum absorption occurs at 700 nm. According to the XRD analysis, Pt/Rutile and Pt/TiO<sub>2</sub> contain 83% and 20% rutile, respectively. However, as Figure 6 demonstrates, the absorption of modified TiO<sub>2</sub> by Mordant increases up to a wavelength of 700 nm, and the best state for modification by this material occurs when Mordant/Pt/TiO<sub>2</sub> is used. Figure 7 shows modification by N<sub>3</sub> and, in this case, the best state of absorption occurs with N<sub>3</sub>/Pt/TiO<sub>2</sub> in the wavelength range 400–600 nm. Figure 8 shows modification by CoPcTs; here the best state of absorption occurs with CoPcTs/Pt/TiO<sub>2</sub> in the wavelength range 600–700 nm.

As Figures 4–8 indicate, in all cases of dye sensitization, maximum absorption in the visible range occurs with dye/Pt/TiO<sub>2</sub> and does not occur with dye/Pt/Rutile. This arises from the smaller size of Pt/TiO<sub>2</sub> nanoparticles compared to Pt/Rutile particles. This characteristic leads to better dispersion of Pt/TiO<sub>2</sub> and, subsequently, better positioning of the dye sensitizer on this substrate.

Table 1: Some characteristics of synthesized samples obtained by BET and XRD analysis.

Sample	Particle size (nm)	Specific surface area (m <sup>2</sup> /g)	Rutile phase percentage
Rutile with calcination temperature of 400 °C	15.4	70	68.3
Rutile with calcination temperature of 450 °C	23.4	65	83
Rutile loaded with platinum (Pt/rutile) at 450 °C	22	65	83
Rutile loaded with platinum and N <sub>3</sub> (N <sub>3</sub> /Pt/Rutile) at 450 °C	23.8	65	83
Commercial TiO <sub>2</sub> loaded with platinum (Pt/TiO <sub>2</sub> -P25)	20.6	50	20
Commercial TiO <sub>2</sub> (TiO <sub>2</sub> -P25)	21	50	20

Figure 5: DRS comparison of TiO<sub>2</sub> loaded with Pt (Pt/TiO<sub>2</sub>) and synthesized Rutile at calcination temperature of 450 °C (rutile) loaded with Pt (Pt/rutile).Figure 6: DRS comparison of TiO<sub>2</sub>, rutile, Pt loaded on TiO<sub>2</sub> (Pt/TiO<sub>2</sub>), and Pt loaded on rutile (Pt/Rutile) modified with Mordant dye.Figure 7: DRS comparison of TiO<sub>2</sub>, rutile, Pt loaded on TiO<sub>2</sub> (Pt/TiO<sub>2</sub>), and Pt loaded on rutile (Pt/Rutile) and modified with N<sub>3</sub> dye.

Finally, as was observed in XRD tests, because of the smaller size of Pt/Rutile nanoparticles compared to dye/Pt/TiO<sub>2</sub> nanoparticles, and the greater surface area of both compared to TiO<sub>2</sub> and Pt/TiO<sub>2</sub>, Pt/Rutile nanoparticles possess maximum absorption in the visible light range and, thereafter, maximum absorption belongs to dye/Pt/TiO<sub>2</sub> materials. The rationalization for this phenomenon was demonstrated through Figure 9. This

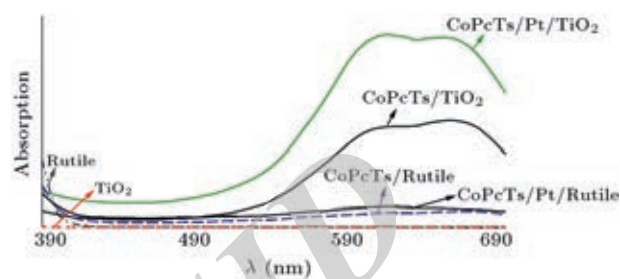
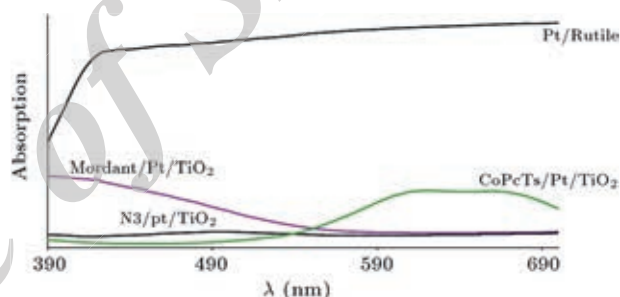
Figure 8: DRS comparison of TiO<sub>2</sub>, rutile, Pt loaded on TiO<sub>2</sub> (Pt/TiO<sub>2</sub>), and Pt loaded on rutile (Pt/Rutile) modified with CoPcTs dye.Figure 9: DRS comparison of Pt/Rutile with different dyes loaded on Pt/TiO<sub>2</sub>.

figure indicates that the Pt/Rutile alone had the smaller size, hence, greater surface area. However, when the dye was loaded onto it, a lower efficiency than dye/Pt/TiO<sub>2</sub> was obtained. Figure 9 also compared the absorption efficiency of different dyes, including Mordant, N<sub>3</sub> and CoPcTs on Pt/TiO<sub>2</sub>, as a template.

#### 4. Conclusions

The best method for modifying the TiO<sub>2</sub> photocatalyst for activation in the visible range was observed with the controlled synthesis of TiO<sub>2</sub> in the rutile phase, with a consequent increase in photocatalytic activity in the visible wavelength range, and also, with the loading of platinum, which causes lagging in the recombination of electron-hole pairs, due to the adsorption of pollutants exposed to light. Another convenient method is the loading of platinum followed by the dye sensitizer precursor as an intermediate in electron transfer from photocatalyst to pollutant, and reduction of the TiO<sub>2</sub> band gap. This study demonstrates the effect of three dye sensitizer precursors, including Mordant, N<sub>3</sub> and CoPcTs, which are utilized to load onto the TiO<sub>2</sub> photocatalyst under visible light irradiation. The synthesized samples were compared with the commercial TiO<sub>2</sub>-P25 material. Evaluation of the effect of calcination temperature on the formation of the nanosize photocatalyst performed by the XRD technique, and the specific surface area, was determined through BET measurements. The efficiencies

of samples were compared using the DRS technique under visible light. This investigation paved the way for preparing and characterizing a nano material to obtain an optimum photocatalytic structure.

## References

- [1] Abdollahi Nejad, B., Sanjabi, S. and Ahmadi, V. "Optical and photocatalytic characteristics of nitrogen doped TiO<sub>2</sub> thin film deposited by magnetron sputtering", *Scientia Iranica*, 17(2), pp. 102–107 (2010).
- [2] Kabra, K., Chaudhary, R. and Sawhney, R.L. "Treatment of hazardous organic and inorganic compounds through aqueous-phase photocatalysis: a review", *Industrial & Engineering Chemistry Research*, 43(24), pp. 7683–7696 (2004).
- [3] Arabatzis, I.M., Spyrellis, N., Loizos, Z. and Falaras, P. "Design and theoretical study of a packed bed photoreactor", *Journal of Materials Processing Technology*, 161, pp. 224–228 (2005).
- [4] Hamerski, M., Grzechulska, J. and Morawski, A.W. "Photocatalytic purification of soil contaminated with using modified TiO<sub>2</sub> powders", *Solar Energy*, 66(6), pp. 395–399 (1999).
- [5] Higarashi, M.M. and Jardim, W.F. "Remediation of pesticide contaminated soil using TiO<sub>2</sub> mediated by solar light", *Catalysis Today*, 76, pp. 201–207 (2002).
- [6] Maira, A.J., Coronado, J.M., Augugliaro, V., Yeung, K.L., Conesa, J.C. and Soria, J. "Fourier transform infrared study of the performance of nanostructured TiO<sub>2</sub> particles for the photocatalytic oxidation of gaseous toluene", *Journal of Catalysis*, 202, pp. 413–420 (2001).
- [7] Medina-Valtierra, J., Garcia-Servin, J., Frausto-Reyes, C. and Calixto, S. "The photocatalytic application and regeneration of anatase thin films with embedded commercial TiO<sub>2</sub> particles deposited on glass microrods", *Applied Surface Science*, 252, pp. 3600–3608 (2006).
- [8] Zhao, X., Quan, X., Zhao, H., Chen, S., Zhao, Y. and Chen, J. "Different effects of humic substances on photodegradation of p, p'-DDT on soil surfaces in the presence of TiO<sub>2</sub> under UV and visible light", *Journal of Photochemistry and Photobiology A: Chemistry*, 167, pp. 177–183 (2004).
- [9] Alexiadis, A. and Mazzarino, I. "Design guidelines for fixed-bed photocatalytic reactors", *Chemical Engineering and Processing*, 44, pp. 453–459 (2005).
- [10] Chen, X. and Mao, S.S. "Titanium dioxide nanomaterials: synthesis, properties, modifications, and applications", *Chemical Reviews*, 107, pp. 2891–2959 (2007).
- [11] Fernandes Machado, N.R.C. and Santana, V.S. "Influence of thermal treatment on the structure and photocatalytic activity of TiO<sub>2</sub> P25", *Catalysis Today*, 107–108, pp. 595–601 (2005).
- [12] O'Regan, B., Moser, J., Anderson, M. and Gratzel, M. "Vectorial electron injection into transparent semiconductor membranes and electric field effects on the dynamics of light-induced charge separation", *Journal of Physical Chemistry*, 94(24), pp. 8720–8726 (1990).
- [13] Mills, A. "Platinisation of semiconductor particles", *Journal of the Chemical Society, Chemical Communications*, 6, pp. 367–368 (1982).
- [14] Bahnemann, D.W., Monig, J. and Chapman, R. "Efficient photocatalysis of the irreversible one-electron and two-electron reduction of halothane on platinized colloidal titanium dioxide in aqueous suspension", *Journal of Physical Chemistry*, 91(14), pp. 3782–3788 (1987).
- [15] Wang, C.M., Heller, A. and Gerischer, H. "Palladium catalysis of O<sub>2</sub> reduction by electrons accumulated on TiO<sub>2</sub> particles during photoassisted oxidation of organic compounds", *Journal of the American Chemical Society*, 114(13), pp. 5230–5234 (1992).
- [16] Driessen, M.D. and Grassian, V.H. "Photooxidation of trichloroethylene on Pt/TiO<sub>2</sub>", *Journal of Physical Chemistry B*, 102(8), pp. 1418–1423 (1998).
- [17] Sclafani, A. and Herrmann, J.-M. "Influence of metallic silver and of platinum-silver bimetallic deposits on the photocatalytic activity of titania (anatase and rutile) in organic and aqueous media", *Journal of Photochemistry and Photobiology A: Chemistry*, 113, pp. 181–188 (1998).
- [18] Einaga, H., Futamura, S. and Ibusuki, T. "Complete oxidation of benzene in gas phase by platinized titania photocatalysts", *Environmental Science and Technology*, 35(9), pp. 1880–1884 (2001).
- [19] Subramanian, V., Wolf, E. and Kamat, P.V. "Semiconductor-metal composite nanostructures, to what extent do metal nanoparticles improve the photocatalytic activity of TiO<sub>2</sub> films?" *Journal of Physical Chemistry B*, 105(46), pp. 11439–11446 (2001).
- [20] Bae, E. and Choi, W. "Highly enhanced photoreductive degradation of perchlorinated compounds on dye-sensitized metal/TiO<sub>2</sub> under visible light", *Environmental Science and Technology*, 37(1), pp. 147–152 (2003).
- [21] Yamakata, A., Ishibashi, T.-A. and Onishi, H. "Water- and oxygen-induced decay kinetics of photogenerated electrons in TiO<sub>2</sub> and Pt/TiO<sub>2</sub>: a time-resolved infrared absorption study", *Journal of Physical Chemistry B*, 105(30), pp. 7258–7262 (2001).
- [22] Hagfeldt, A. and Graetzel, M. "Light-induced redox reactions in nanocrystalline systems", *Chemical Reviews*, 95(1), pp. 49–68 (1995).
- [23] Pirkanniemi, K. and Sillanpaa, M. "Heterogeneous water phase catalysis as an environmental application: a review", *Chemosphere*, 48, pp. 1047–1060 (2002).
- [24] Zaban, A., Ferrere, S., Sprague, J. and Gregg, B.A. "pH-dependent redox potential induced in a sensitizing dye by adsorption onto TiO<sub>2</sub>", *Journal of Physical Chemistry B*, 101(1), pp. 55–57 (1997).
- [25] Chao, C.-H., Chang, C.-L., Chan, C.-H., Lien, S.-Y., Weng, K.-W. and Yao, K.-S. "Rapid thermal melted TiO<sub>2</sub> nano-particles into ZnO nano-rod and its application for dye sensitized solar cells", *Thin Solid Films*, 518, pp. 7209–7212 (2010).
- [26] Banerjee, A.N. "The design, fabrication, and photocatalytic utility of nanostructured semiconductors: focus on TiO<sub>2</sub>-based nanostructures", *Nanotechnology, Science and Applications*, 4, pp. 35–65 (2011).
- [27] Bosc, F., Ayrat, A., Keller, N. and Keller, V. "Room temperature visible light oxidation of CO by high surface area rutile TiO<sub>2</sub>-supported metal photocatalyst", *Applied Catalysis B: Environmental*, 69, pp. 133–137 (2007).
- [28] Steward, G.C. "Diffuse reflectance spectroscopy for the characterization of calcareous glacial till soils from north central montana", M.Sc. Thesis, Montana State University (2006).
- [29] Panagiotopoulou, P. and Kondarides, D.I. "Effect of morphological characteristics of TiO<sub>2</sub>-supported noble metal catalysts on their activity for the water-gas shift reaction", *Journal of Catalysis*, 225, pp. 327–336 (2004).
- [30] Ishibai, Y., Sato, J., Nishikawa, T. and Miyagishi, S. "Synthesis of visible-light active TiO<sub>2</sub> photocatalyst with Pt-modification: role of TiO<sub>2</sub> substrate for high photocatalytic activity", *Applied Catalysis B: Environmental*, 79, pp. 117–121 (2008).
- [31] Koci, K., Obalova, L., Matejova, L., Placha, D., Lacny, Z., Jirkovsky, J. and Solcova, O. "Effect of TiO<sub>2</sub> particle size on the photocatalytic reduction of CO<sub>2</sub>", *Applied Catalysis B: Environmental*, 89, pp. 494–502 (2009).
- [32] Vijayabalan, A., Selvam, K., Velmurugan, R. and Swaminathan, M. "Photocatalytic activity of surface fluorinated TiO<sub>2</sub>-P25 in the degradation of reactive orange 4", *Journal of Hazardous Materials*, 172, pp. 914–921 (2009).

**Hoda Sadat Mazloomi Tabaei** obtained her B.S. degree in Chemical Engineering from the University of Tehran, Iran, and M.S. degree in Chemical Engineering from the Department of Chemical and Petroleum Engineering at Sharif University of Technology, Tehran, Iran. Her research interests include catalyst preparation, characterization and evaluation in the field of chemical engineering.

**Mohammad Kazemeini** is Professor of Chemical and Petroleum Engineering at Sharif University of Technology, Tehran, Iran. Currently, his main research interests include nano-catalysts (mostly, CNT and CNF based) preparation, characterization and evaluation in the field of Petroleum Refining.

**Moslem Fattahi** obtained his B.S. degree in Chemical Engineering from Razi University, Kermanshah, Iran, and his M.S. degree from the Department of Chemical and Petroleum Engineering at Sharif University of Technology, Tehran, Iran. His main research interests include modeling and reaction engineering, catalyst preparation, characterization and evaluation in the field of chemical engineering.